

Crystal and molecular structures of 2-[1-(2-aminoethyl)-2-imidazolidinylidene]-2-nitroacetonitrile (C₇H₁₁N₅O₂) and 2,6-diamino-5-hydroxy-3-nitro-4H-pyrazolo[1,5-a]pyrimidin-7-one monohydrate (C₆H₆N₆O₄·H₂O) from X-ray, synchrotron and neutron powder diffraction data

V. V. CHERNYSHEV,^{a*} A. N. FITCH,^b E. J. SONNEVELD,^c A. I. KURBAKOV,^d V. A. MAKAROV^e AND V. A. TAFEENKO^a

^aMoscow State University, Department of Chemistry, 119899 Moscow, Russia, ^bESRF, BP 220, F-38043, Grenoble CEDEX, France, ^cUniversity of Amsterdam, Laboratory of Crystallography, Nieuwe Achtergracht 166, Amsterdam 1018 WV, The Netherlands, ^dNuclear Physics Institute of the Russian Academy of Sciences, 188350 Gatchina, Russia, and ^eState Scientific Center 'NIOPIK', Department of Medicinal Chemistry, B. Sadovaya Street 1–4, 103787 Moscow, Russia. E-mail: cher@biocryst.phys.msu.su

(Received 8 October 1998; accepted 2 February 1999)

Abstract

The crystal and molecular structures of 2-[1-(2-aminoethyl)-2-imidazolidinylidene]-2-nitroacetonitrile [C₇H₁₁N₅O₂; space group $P2_1/n$; $Z = 4$; $a = 7.4889$ (8), $b = 17.273$ (2), $c = 7.4073$ (8) Å, $\beta = 111.937$ (6)°], (I), and 2,6-diamino-5-hydroxy-3-nitro-4H-pyrazolo[1,5-a]pyrimidin-7-one monohydrate [C₆H₆N₆O₄·H₂O; space group $P2_1/n$; $Z = 4$; $a = 17.576$ (3), $b = 10.900$ (2), $c = 4.6738$ (6) Å, $\beta = 92.867$ (8)°], (II), have been determined from X-ray, synchrotron and neutron powder diffraction data using various methods. The structures were originally solved from Guinier photographs with a grid search procedure and the program *MRIA* using *a priori* information from NMR and mass spectra on the possible geometry of the molecules. Because the conformation of molecule (I) changed during the bond-restrained Rietveld refinement, solvent water was found in (II) and, moreover, as both Guinier patterns were corrupted by texture, high-resolution texture-free synchrotron data were collected at the BM16 beamline, ESRF, to confirm the original results. Using the set of $|F|^2$ values derived from the synchrotron patterns after full-pattern decomposition procedures, the structures of (I) and (II) were solved by direct methods via *SHELXS96*, *SIRPOW.92* and *POWSIM* without any preliminary models of the molecules, and by Patterson search methods via *DIRDIF96* and *PATSEE* with the use of rigid fragments from each of the molecules. The neutron patterns allowed (I) and (II) to be solved using the grid search procedure and correct initial models of the molecules including H atoms. The results obtained from powder patterns measured on different devices demonstrate the high level of reproducibility and reliability of various powder software and equipment, with a certain preference for synchrotron facilities.

1. Introduction

Powder diffraction methods play an important role in the characterization of new organic materials which can only be prepared in polycrystalline form. The number of molecular organic crystal structures solved *ab initio* from powder data is increasing steadily (Giacovazzo, 1996; Dinnebier *et al.*, 1997; Poojary & Clearfield, 1997; LeBail, 1998). A wide and varied range of methods and software is now available for structure solution from powder data. In some cases one may find the solution by use of routine direct methods and high-resolution synchrotron data. On the other hand, the presence of only light atoms reduces the number of high-angle reflections considerably, making the application of direct methods very difficult when using low-resolution laboratory data. The overlap of diffraction peaks, accidental or systematic, and preferred-orientation effects are further complications. However, information about the structure combined with the Patterson search method (Rius & Miravittles, 1987, 1988), the Monte Carlo technique (Tremayne *et al.*, 1996), genetic algorithms (Shankland *et al.*, 1997; Harris *et al.*, 1998), simulated annealing (David *et al.*, 1998) or the grid search procedure (Chernyshev & Schenk, 1998) can often help in solving molecular crystal structures. Increasing degrees of freedom, presumptions and applied corrections in crystal structure determination from low-resolution powder data generate the problem of reliability and reproducibility of the results obtained with different software. The present work is an attempt to investigate this problem in terms of the solutions of two unknown molecular crystal structures – [2-[1-(2-aminoethyl)-2-imidazolidinylidene]-2-nitroacetonitrile, C₇H₁₁N₅O₂, (I), and 2,6-diamino-5-hydroxy-3-nitro-4H-pyrazolo[1,5-a]pyrimidin-7-one monohydrate, C₆H₆N₆O₄·H₂O, (II). Compound (I) belongs to the

Table 1. *Crystal data*

	(I)	(II)
Formula	C ₇ H ₁₁ N ₅ O ₂	C ₆ H ₆ N ₆ O ₄ ·H ₂ O
System	Monoclinic	Monoclinic
Space group	<i>P</i> 2 ₁ / <i>n</i>	<i>P</i> 2 ₁ / <i>n</i>
<i>a</i> (Å)	7.4889 (8)	17.576 (3)
<i>b</i> (Å)	17.273 (2)	10.900 (2)
<i>c</i> (Å)	7.4073 (8)	4.6738 (6)
β (°)	111.937 (6)	92.867 (8)
<i>M</i> ₂₀	192	148
<i>V</i> (Å ³)	888.8 (2)	894.3 (3)
<i>Z</i>	4	4
<i>D</i> _x (g cm ⁻³)	1.474	1.814

family of Ranitidine-related compounds of imidazolidine type containing a methylene group. The investigation of their possible conformations allows the study of the properties of the H₁-receptor blocker. Compound (II) is representative of 3-amino-4-nitro-7-oxopyrazolo[1,5-*a*]pyrimidine derivatives which demonstrate antiphlogistic and anti-inflammatory activity in α -hydrosteroid dehydrogenase (α -HSD) tests. The level of their activity is comparable with the activities of Ibuprofen and Indomethacin.

2. Experimental and data analysis

2.1. Synthesis

Compound (I): A solution of 2.00 g (17.4 mmol) of 2-nitro-2-cyano-1-dimethylaminoenamine and 2.00 g (19.2 mmol) of 2-(2-aminoethyl)ethanol in 60 ml of 2-propanol was refluxed for 5 h. The reaction mixture was cooled and filtered to collect the colourless fine polycrystals. The yield was 2.36 g (91%) from 2-propanol. M.p. 407–409 K. *M*⁺ = 198.18. ¹H-NMR [DMSO-*d*₆, δ (p.p.m.)]: 3.06 (2H, *t*, CH₂ ethylene), 3.65 (2H, *t*, CH₂ ethylene), 3.97 (2H, *t*, CH₂ imidazolidine), 4.15 (2H, *t*, CH₂ imidazolidine). Analysis: found C 42.13, H 4.76, N 28.31; C₇H₁₁N₅O₂ requires C 42.42, H 5.09, N 28.27%.

Compound (II): A mixture of 2.00 g (14.0 mmol) of 3,5-diamino-4-nitropyrazole with 3.03 g (14.0 mmol) diethyl acetamidomalonate and 1 ml (7.2 mmol) triethylamine in 60 ml of ethanol was refluxed for 4 h. The reaction mass was cooled, 10 ml of 2 *M* hydrochloric acid was added and the mixture was refluxed again for 6 h. The suspension was then cooled in the refrigerator and filtered to collect yellow polycrystals. The yield was 2.84 g (86%) from acetic acid. M.p. 519–521 K. *M*⁺ = 226.15. Analysis: found C 31.83, H 2.54, N 37.45; C₆H₆N₆O₄·H₂O requires C 31.87, H 2.67, N 37.16%.

2.2. Unit-cell parameters and space-group determination

The monoclinic cell dimensions of (I) and (II) were determined first from Guinier photographs by the indexing programs *ITO* (Visser, 1969), *TREOR*90 (Werner *et al.*, 1985) and *AUTOX* (Zlokazov, 1992)

using more than 45 peak positions. A small number of very weak lines from impurities was observed for (I) (*d* spacings: 6.760, 6.555 and 5.950 Å). The space group *P*2₁/*n* was determined for (I) and (II) on the basis of systematic extinction rules. The unit-cell parameters and space groups were confirmed further by synchrotron measurements and the unit-cell parameters were refined with the program *LSPAID* (Visser, 1986) using 50 low-angle peak positions extracted from the synchrotron patterns. Crystal data for (I) and (II) are summarized in Table 1.

2.3. Data collection

All patterns were measured at room temperature. Guinier photographs (Table 2) were taken in transmission mode with an Enraf–Nonius Guinier–Johannson FR552 camera using quartz monochromated Cu *K* α ₁ radiation. Intensities were collected in 0.01° steps using a Johannson LS18 line scanner. The camera was evacuated to avoid air scattering. The specimens were prepared by pressing each powder onto Mylar foil to form a thin layer. Because of this preparation procedure preferred orientation is likely to occur; indeed, considerable preferred orientation was observed for the two compounds. During the measurements each specimen was spun in the specimen plane.

Synchrotron X-ray diffraction measurements (Table 2) were carried out at the powder diffraction beamline BM16 at the ESRF, Grenoble, France. Sample (I) was sealed in a 1 mm diameter borosilicate glass capillary and diffraction data were collected at a wavelength λ of 0.85617 (3) Å over a period of 12 h. Sample (II), which has a more feathery appearance, was sealed in a 1.5 mm diameter capillary and data were collected at λ = 0.95044 (2) Å for 6 h. In each case the capillary was spun on the axis of the diffractometer while the bank of nine detectors and Ge(111) analyser crystals was scanned at a rate of 0.5° min⁻¹. The 2 θ encoder and the electronic scalers were read every 200 ms. The high-angle regions of the pattern were scanned more frequently than the low-angle regions to improve the statistical quality of the data. The counts acquired from the nine detectors during various scans were combined to yield the equivalent step scans, with a step of 0.004 and 0.005° for samples (I) and (II), respectively.

Neutron powder diffraction experiments (Table 2) were carried out on the high-resolution multi-counter powder diffractometer (HRMCPD, Petersburg Nuclear Physics Institute) situated at the Orphee reactor of the Leon Brillouin Laboratory. Data collection for samples (I) and (II) took 36 and 34 h, respectively.

2.4. Structure solution and refinement

The full-pattern decomposition procedures and bond-restrained Rietveld refinements (Table 2) were performed with the updated *MRIA* program (Zlokazov

Table 2. *The powder diffraction data sets*

$R_B = \sum |y_o - y_c| / \sum |y_o - \text{background}|$, $R_p = \sum |y_o - y_c| / \sum y_o$ and $R_{\text{exp}} = \sum \sigma y_o / \sum y_o$, where y_o and y_c are the observed and calculated intensities at each point of the pattern. The sum for R_B , R_p and R_{exp} is over all points of the pattern. The results of the full-pattern decomposition procedure are given in the first line of each pair and the results of the final bond-restrained Rietveld refinement are given in the second line of each pair.

Pattern	Compound (I)			Compound (II)		
	I.1	I.2	I.3	II.1	II.2	II.3
Instrument	Guinier camera	BM16, ESRF	HRMCPD, LLB	Guinier camera	BM16, ESRF	HRMCPD, LLB
Wavelength, λ (Å)	1.54059	0.85617 (3)	2.8249	1.54059	0.95044 (2)	2.3433
2θ (°)	8–60	4–44	10–150	8–80	5–55	10–154
2θ step (°)	0.01	0.004	0.1	0.01	0.005	0.1
No. of reflections	255	629	295	542	861	534
$(\sin \theta / \lambda)_{\text{max}}$ (Å ⁻¹)	0.325	0.438	0.342	0.417	0.486	0.406
χ^2	5.0	1.9	1.8	6.2	3.1	2.6
	5.6	2.1	1.9	6.3	3.0	3.2
R_p (%)	6.1	5.0	0.9	5.6	5.5	1.0
	6.8	5.1	0.9	5.9	5.7	1.2
R_B (%)	13.6	16.5	15.8	11.6	9.9	10.3
	15.0	17.6	17.9	12.0	10.1	12.4
R_{exp} (%)	3.5	4.0	0.9	2.8	3.6	0.9

& Chernyshev, 1992). All patterns were fitted using a split pseudo-Voigt peak profile function (Toraya, 1986). The strong anisotropy of diffraction-line broadening, observed in all patterns of (II) and particularly in the synchrotron pattern, was approximated by a quartic form in hkl [Popa, 1998; expression (7)] with nine variables. March–Dollase (Dollase, 1986) and symmetrized harmonics expansion (Ahtee *et al.*, 1989; Järvinen, 1993) texture formalisms were used when processing textured patterns. The background was approximated by a Chebyshev polynomial. All s.u.'s were multiplied by a factor calculated by a program module which estimates probable errors obtained in Rietveld refinements with serial correlations (Bérar & Lelann, 1991); the factor varied between 1.5 and 2 for different patterns.†

2.4.1. *Guinier patterns.* Preliminary information about the possible structures of (I) and (II) (Fig. 1) was obtained from IR and NMR spectroscopy, and mass spectrometry. The initial models of the molecules were built up with the program *MOPAC6.0* (Stewart, 1990).

Compound (I): All the initial planar models (I)-A–(I)-C (Fig. 1) were tested with the grid search procedure (Chernyshev & Schenk, 1998) in an attempt to locate the molecule in the asymmetric part of the unit cell. The grid increments were taken as 0.6 Å for molecule translations along **a**, **b** and **c** and 20° for the three rotations. 14 non-H atoms with an overall displacement factor $U_{\text{iso}} = 0.05 \text{ \AA}^2$ were used in a search for the best molecular position, fitting to 70 low-angle X_{obs} values derived from the Guinier pattern after the full-pattern decomposition

procedure (Table 2). X_{obs} is proportional to the intensity of the group of overlapping peaks and is written as (Chernyshev & Schenk, 1998)

$$X_{\text{obs}} = \sum_i m_i |F_{\text{obs},i}|^2,$$

where the summation is over the overlapping reflections and m_i is the multiplicity of the i th reflection. Because models *B* and *C* gave no minimum of $R(X)$ less than 70% they were rejected from subsequent considerations. Model *A* provided $R(X) = 57\%$ and was used as a starting model in the bond-restrained Rietveld refinement (Fig. 2a). Multi-component symmetrized harmonics (up to the sixth order) expansion was used to take into account preferred-orientation effects. The largest texture-correction multiplier, 1.58, was applied to the intensity of the 080 reflection and the lowest one, 0.39, was applied to the intensity of the 110 reflection. During the bond-restrained Rietveld refinement with gradually relaxed (but not rejected) distance requirements, the conformation of the initially planar molecule *A* changed considerably as the amino group and the adjacent C atom moved out of the plane of the molecule. The atomic coordinates obtained are given in Table 3 on the first line for each atom.

Compound II: The initial models (II)-A–(II)-C (Fig. 1) are qualitatively equivalent. Therefore, only model *C* was used in the grid search procedure, with grid increments as for (I). The minimum of $R(X) = 52\%$ was observed for 100 low-angle X_{obs} values and 16 non-H atoms. The resulting molecular position was used as the initial position in subsequent bond-restrained Rietveld refinement. The March–Dollase texture formalism with [100] as the direction of preferred orientation was

† Supplementary data for this paper are available from the IUCr electronic archives (Reference: AN0555). Services for accessing these data are described at the back of the journal.

applied. However, the value of χ^2 obtained was not less than 65, compared with $\chi^2 = 6.2$ obtained in the full-pattern decomposition procedure (Table 2). Therefore, a difference Fourier map was calculated with *SHELXL93* (Sheldrick, 1993) on the basis of 107 reflections derived from 100 X_{obs} values with equal partitioning of overlapping reflections. The $|F_{\text{obs}}|^2$ values were corrected for texture by setting the March–Dollase texture parameter r to 1.3. A single peak far from the molecule was found. It was assigned to the O atom of the solvent water molecule and refined together with the initial molecule. χ^2 dropped to 6.3 (Table 2) and the molecule refined to structure *A* (Fig. 1). The atomic coordinates are given in Table 4 on the first line for each atom. The texture parameter r refined to 1.58 (1).

2.4.2. Synchrotron patterns. Synchrotron radiation from the third-generation synchrotron source ESRF, because of its high brightness and excellent vertical collimation, provides high-resolution X-ray powder data with minimal peak overlap. By working in transmission geometry with the sample contained in a spinning capillary 1 or 1.5 mm in diameter, preferred orientation can be minimized. The intensities of 629 and 861 reflections for (I) and (II), respectively, were derived from the synchrotron patterns with the full-pattern decomposition procedure (Table 2). The intensities of overlapping reflections were equally partitioned.

Two sets of $|F_{\text{obs}}|^2$ values were used in the crystal structure determination with *DIRDIF96* (Beurskens *et al.*, 1996) and *PATSEE* (Egert & Sheldrick, 1985), programs which effectively exploit the known geometry of a molecular fragment. For (I) the common part of the structures *A* and *B* (Fig. 1) – 11 non-H atoms without the amino group and two C atoms – was chosen, and for (II) the common part of the structures *A–C*, containing 13 non-H atoms, was chosen. Both programs found the same solutions for (I) and (II) in a standard run. Moreover, the high quality of the synchrotron data

allowed us to obtain the same crystal structure solutions with direct methods using *SHELXS96* (Sheldrick, 1990), *SIRPOW.92* (Altomare *et al.*, 1994) and *POWSIM* (*SIMPEL* algorithm; Overbeek & Schenk, 1978) without any preliminary models of the molecules. The positions of the two H atoms of the water molecule in (II) were found in a difference Fourier map calculated with *SHELXL93*.

The atomic coordinates obtained from the synchrotron patterns after bond-restrained Rietveld refinement for (I) (Fig. 2*b*) and (II) (Fig. 3*b*) are given in the second lines of Tables 3 and 4 for each atom, respectively. The March–Dollase texture parameters r for (I) and (II) refined to 1.066 (4) and 1.053 (3), respectively.

2.4.3. Neutron patterns. As usual for neutron measurements, sample-preparation procedures allowed us to avoid preferred orientation effects for (I), but not for (II), therefore no texture correction was applied while processing the neutron pattern I.3.

Compound (I): The solution was found with the grid search procedure only. The correct, non-planar, structure (I)-*A* (Fig. 1) including the H atoms – 25 atoms in total – was used for translational and rotational search on the basis of 75 low-angle X_{obs} values containing the intensities of 103 reflections derived from the neutron pattern I.3 (Table 2). The grid increments were the same as those used for the Guinier pattern. The minimum of $R(X) = 48\%$ was clearly discriminated from the next minimum at 55%. The molecular position obtained was used in subsequent bond-restrained Rietveld refinement (Fig. 2*c*), which led to the atomic coordinates given in the third lines of Table 3 for each atom.

Compound (II): The correct solution was again found with the grid search procedure only. The structure (II)-*A* (Fig. 1) – 22 atoms in total – was used for the translational and rotational search, fitting to 75 low-angle X_{obs} values (87 reflections) derived from the pattern II.3 (Table 2). The minimum of $R(X) = 51\%$ provided the

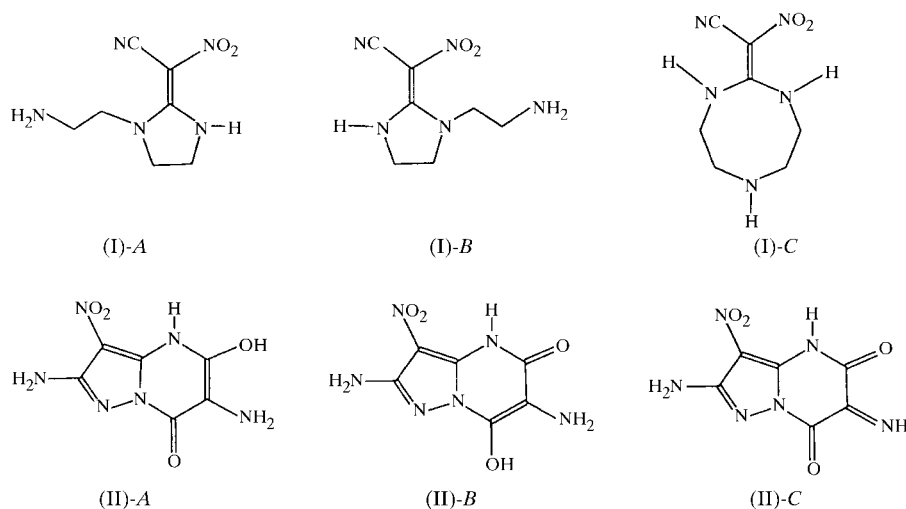


Fig. 1. Chemical diagrams for the initial models of the molecules of (I) and (II).

Table 3. Atomic coordinates and isotropic displacement parameters (\AA^2) for (I) after the final bond-restrained Rietveld refinement

Results from the X-ray pattern I.1, the synchrotron pattern I.2 and the neutron pattern I.3 are given in the first, second and third lines for each atom, respectively. An overall U_{iso} was refined for the H atoms. An overall U_{iso} for the non-H atoms was refined in the case of the X-ray pattern.

	<i>x</i>	<i>y</i>	<i>z</i>	U_{iso}
O1	0.211 (1) 0.2150 (8) 0.220 (4)	0.6298 (6) 0.6302 (3) 0.633 (2)	0.375 (1) 0.3818 (9) 0.371 (4)	0.057 (1) 0.065 (6) 0.11 (3)
O2	0.468 (1) 0.4715 (7) 0.464 (4)	0.5889 (4) 0.5869 (3) 0.591 (2)	0.3416 (6) 0.3457 (9) 0.332 (4)	0.057 0.070 (6) 0.10 (3)
N1	0.459 (2) 0.4562 (8) 0.447 (3)	0.4468 (6) 0.4475 (3) 0.446 (1)	0.198 (2) 0.185 (1) 0.182 (2)	0.057 0.032 (4) 0.07 (1)
N2	0.199 (2) 0.2009 (7) 0.200 (2)	0.3763 (7) 0.3757 (3) 0.372 (1)	0.149 (2) 0.1460 (8) 0.147 (2)	0.057 0.048 (5) 0.08 (1)
N3	0.149 (2) 0.1403 (8) 0.149 (2)	0.3142 (7) 0.3163 (3) 0.311 (1)	0.502 (2) 0.5002 (7) 0.513 (2)	0.057 0.057 (5) 0.05 (1)
N4	0.300 (2) 0.3019 (9) 0.308 (3)	0.5779 (6) 0.5788 (4) 0.577 (1)	0.343 (2) 0.334 (1) 0.340 (3)	0.057 0.043 (5) 0.05 (1)
N5	-0.155 (1) -0.1526 (8) -0.146 (3)	0.5113 (7) 0.5103 (3) 0.509 (2)	0.251 (2) 0.253 (1) 0.262 (3)	0.057 0.063 (5) 0.09 (2)
C2	0.282 (2) 0.2798 (8) 0.274 (3)	0.4460 (9) 0.4461 (3) 0.443 (1)	0.215 (2) 0.205 (1) 0.205 (2)	0.057 0.050 (6) 0.05 (1)
C3	0.509 (2) 0.5080 (9) 0.508 (3)	0.372 (1) 0.3741 (4) 0.369 (1)	0.140 (2) 0.126 (1) 0.130 (3)	0.057 0.069 (7) 0.04 (1)
C4	0.314 (2) 0.3237 (8) 0.313 (4)	0.3289 (9) 0.3276 (3) 0.329 (1)	0.072 (2) 0.0779 (9) 0.069 (3)	0.057 0.081 (7) 0.08 (2)
C5	0.197 (2) 0.1975 (8) 0.200 (3)	0.5108 (8) 0.5107 (3) 0.508 (1)	0.256 (2) 0.257 (1) 0.257 (4)	0.057 0.032 (5) 0.07 (2)
C6	-0.001 (2) 0.0017 (9) 0.008 (3)	0.5079 (9) 0.5084 (3) 0.506 (1)	0.258 (2) 0.255 (1) 0.256 (4)	0.057 0.026 (4) 0.07 (2)
C7	0.013 (2) 0.0181 (8) 0.020 (3)	0.343 (1) 0.3423 (3) 0.336 (1)	0.137 (2) 0.1388 (8) 0.154 (3)	0.057 0.072 (7) 0.02 (1)
C8	0.042 (2) 0.0489 (8) 0.071 (3)	0.287 (1) 0.2865 (3) 0.281 (1)	0.306 (2) 0.3077 (9) 0.320 (4)	0.057 0.054 (6) 0.08 (1)
H1	0.54 (1) 0.525 (6)	0.491 (6) 0.495 (3)	0.22 (1) 0.188 (6)	0.06 (3) 0.12 (3)

Table 3 (cont.)

	<i>x</i>	<i>y</i>	<i>z</i>	U_{iso}
	0.535 (6)	0.491 (3)	0.207 (6)	0.11 (1)
H3	0.61 (1) 0.612 (7) 0.609 (7)	0.347 (5) 0.352 (3) 0.355 (3)	0.25 (1) 0.235 (7) 0.252 (6)	0.06 0.12 0.11
H31	0.55 (1) 0.548 (8) 0.545 (7)	0.376 (6) 0.378 (3) 0.384 (3)	0.04 (1) 0.017 (6) 0.011 (6)	0.06 0.12 0.11
H4	0.26 (1) 0.265 (8) 0.250 (7)	0.324 (5) 0.320 (3) 0.325 (2)	-0.06 (1) -0.063 (6) -0.075 (6)	0.06 0.12 0.11
H41	0.33 (1) 0.345 (8) 0.330 (6)	0.279 (6) 0.279 (3) 0.277 (3)	0.13 (1) 0.145 (6) 0.118 (5)	0.06 0.12 0.11
H7	-0.05 (1) -0.042 (8) -0.049 (6)	0.317 (5) 0.315 (3) 0.311 (2)	0.02 (1) 0.018 (7) 0.022 (6)	0.06 0.12 0.11
H71	-0.07 (1) -0.068 (7) -0.073 (7)	0.385 (5) 0.384 (3) 0.379 (2)	0.14 (1) 0.140 (7) 0.144 (6)	0.06 0.12 0.11
H8	-0.08 (1) -0.079 (7) -0.066 (6)	0.273 (6) 0.272 (3) 0.271 (3)	0.30 (1) 0.301 (6) 0.314 (6)	0.06 0.12 0.11
H81	0.10 (1) 0.115 (6) 0.143 (6)	0.243 (5) 0.242 (3) 0.237 (3)	0.28 (1) 0.290 (7) 0.303 (6)	0.06 0.12 0.11
H9	0.14 (1) 0.141 (6) 0.161 (7)	0.366 (6) 0.369 (3) 0.368 (2)	0.54 (1) 0.535 (6) 0.535 (6)	0.06 0.12 0.11
H91	0.23 (1) 0.230 (7) 0.262 (6)	0.279 (6) 0.283 (3) 0.291 (3)	0.60 (1) 0.601 (6) 0.611 (6)	0.06 0.12 0.11

initial model for the subsequent Rietveld refinement (Fig. 3c). The positions of the O atom and the two H atoms of the water molecule were found in a difference Fourier map. The final atomic coordinates are given in third lines of Table 4 for each atom. The March–Dollase texture parameter r refined to 1.15 (1).

3. Discussion

3.1. Crystal and molecular structures

The crystal packings of (I) and (II) were analysed with the program *PLUTON92* (Spek, 1992) using atomic coordinates derived from the synchrotron patterns. Figs. 4 and 5 were also prepared with *PLUTON92*.

The molecular structure of compound (I) is shown in Fig. 4. The molecules in the crystal are connected by van

der Waals interactions; no intermolecular hydrogen bonds were found.

The crystal-packing motif of compound (II) with the atomic numbering is presented in Fig. 5. The four molecules in one unit cell form two centrosymmetric dimers by means of hydrogen bonds involving the amino and hydroxy groups. The parameters of the hydrogen bonds are $\text{H3}\cdots\text{N1}'$ 2.10 (5) Å, $\text{N3}-\text{H3}\cdots\text{N1}'$ 143 (4)° and $\text{H5}\cdots\text{O2}''$ 1.91 (5) Å, $\text{N5}-\text{H5}\cdots\text{O2}''$ 162 (4)°. The chains of molecules obtained are related through intermolecular hydrogen bonds [$\text{H61}\cdots\text{O4}'''$ 1.81 (5) Å, $\text{N6}-\text{H61}\cdots\text{O4}'''$ 160 (4)°, $\text{H7}\cdots\text{N6}''''$ 2.12 (5) Å, $\text{O2}-\text{H7}\cdots\text{N6}''''$ 156 (4)°] and hydrogen bonds with the water molecule [$\text{H6}\cdots\text{O5}$ 1.83 (5) Å, $\text{N6}-\text{H6}\cdots\text{O5}$ 162 (4)°] (symmetry codes: ' $1-x, -y, 1-z$; '' $1-x, 1-y, -1-z$; ''' $-\frac{1}{2}+x, \frac{1}{2}-y, \frac{1}{2}+z$; '''' $x, y, -1+z$).

3.2. Reproducibility of the results

The important result of the present work is the high level of reproducibility of the atomic coordinates for (I) and (II) obtained from various powder patterns (Tables 3 and 4). Even a considerable preferred-orientation effect observed in Guinier patterns I.1 and II.1 was successfully taken into account during the crystal structure solution. This conclusion supports confidence in the accuracy of the results of crystal structure solution from laboratory powder data with strong texture (Yatsenko *et al.*, 1999). Of course, the use of bond restraints in the Rietveld refinement – although very

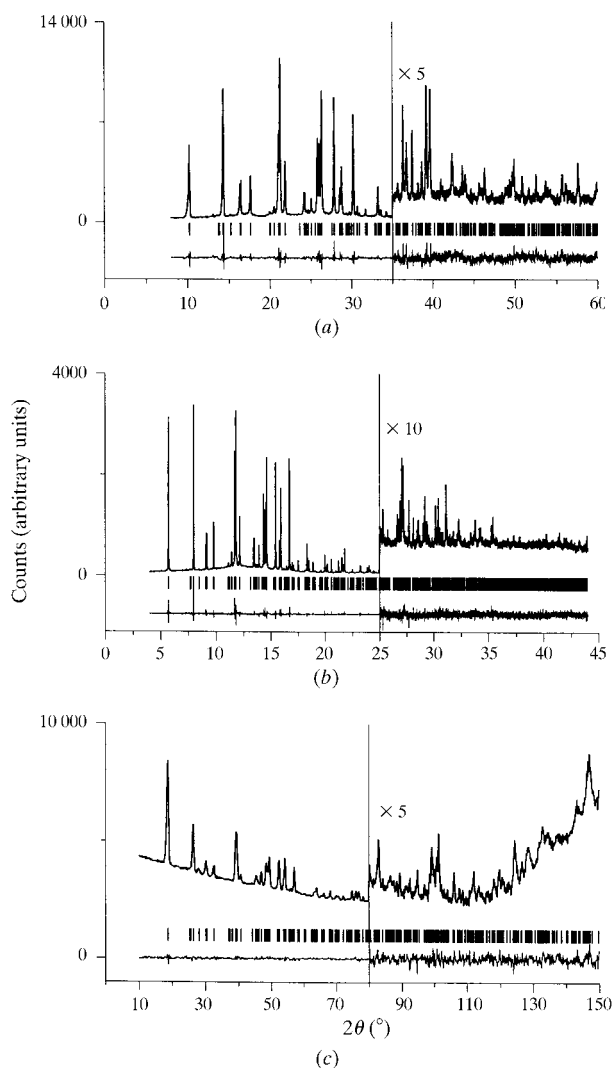


Fig. 2. Rietveld plots for (I): (a) Guinier pattern I.1; (b) synchrotron pattern I.2; (c) neutron pattern I.3 (a constant background has been subtracted from the scaled high-angle part of the plot).

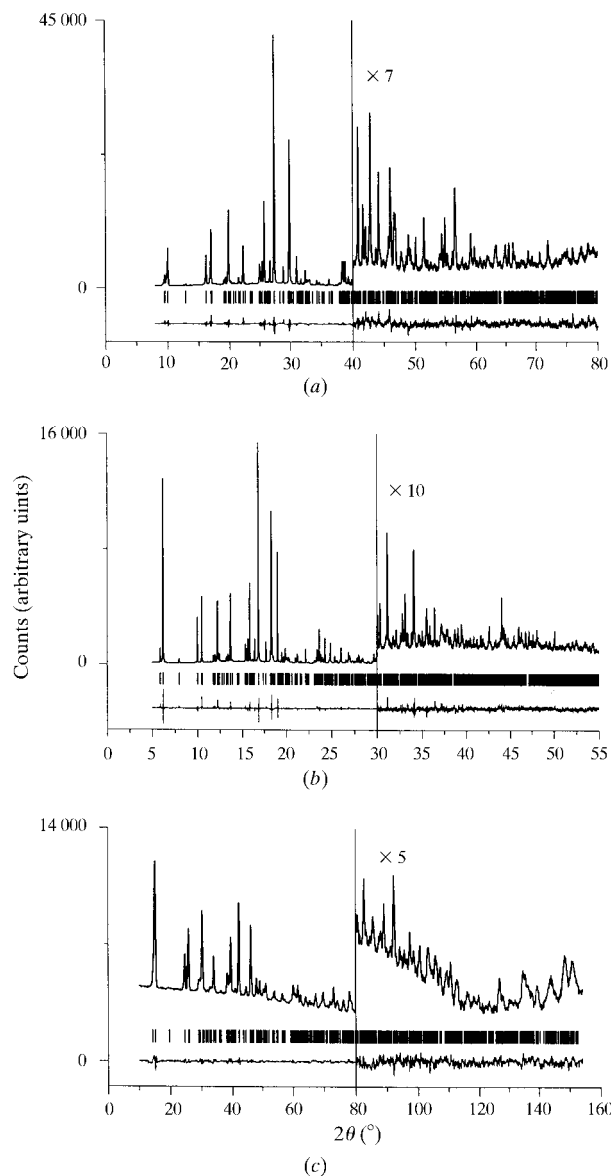


Fig. 3. Rietveld plots for (II): (a) Guinier pattern II.1; (b) synchrotron pattern II.2; (c) neutron pattern II.3 (a constant background has been subtracted from the scaled high-angle part of the plot).

Table 4. Atomic coordinates and isotropic displacement parameters (\AA^2) for (II) after the final bond-restrained Rietveld refinement

Results from the X-ray pattern II.1, the synchrotron pattern II.2 and the neutron pattern II.3 are given in the first, second and third lines for each atom, respectively. Eight isotropic displacement parameters were refined: six parameters for O1–O5 and N4, an overall U_{iso} for the other non-H atoms and an overall U_{iso} for the H atoms.

	<i>x</i>	<i>y</i>	<i>z</i>	U_{iso}
O1	0.3616 (4) 0.3574 (2) 0.348 (2)	0.2520 (4) 0.2495 (3) 0.251 (2)	0.394 (1) 0.3957 (8) 0.396 (5)	0.033 (2) 0.013 (1) 0.03 (1)
O2	0.4178 (3) 0.4173 (2) 0.419 (2)	0.5223 (4) 0.5256 (3) 0.525 (3)	−0.3421 (8) −0.3330 (8) −0.342 (7)	0.017 (2) 0.019 (2) 0.09 (2)
O3	0.6437 (4) 0.6433 (2) 0.647 (2)	0.2662 (4) 0.2693 (3) 0.271 (2)	−0.375 (1) −0.3727 (8) −0.367 (5)	0.042 (3) 0.022 (3) 0.03 (1)
O4	0.6907 (4) 0.6913 (2) 0.695 (2)	0.1063 (4) 0.1096 (3) 0.118 (3)	−0.1366 (9) −0.1366 (8) −0.131 (7)	0.031 (2) 0.025 (2) 0.10 (2)
O5	0.2461 (4) 0.2484 (3) 0.250 (2)	0.6432 (4) 0.6438 (3) 0.652 (2)	−0.236 (1) −0.237 (1) −0.217 (5)	0.030 (2) 0.020 (2) 0.02 (1)
N1	0.4930 (5) 0.4909 (3) 0.488 (1)	0.1275 (5) 0.1227 (4) 0.121 (1)	0.297 (1) 0.293 (1) 0.290 (3)	0.026 (1) 0.010 (1) 0.039 (4)
N2	0.4663 (5) 0.4644 (3) 0.466 (1)	0.2281 (5) 0.2226 (4) 0.221 (1)	0.139 (1) 0.1357 (8) 0.134 (3)	0.026 0.010 0.039
N3	0.6011 (5) 0.6025 (3) 0.603 (1)	−0.0013 (5) 0.0020 (4) −0.001 (2)	0.280 (1) 0.2864 (9) 0.288 (3)	0.026 0.010 0.039
N4	0.6393 (5) 0.6403 (3) 0.642 (1)	0.1787 (6) 0.1871 (4) 0.189 (1)	−0.194 (1) −0.1899 (9) −0.187 (3)	0.047 (3) 0.020 (2) 0.05 (1)
N5	0.4997 (5) 0.4948 (3) 0.492 (1)	0.3654 (5) 0.3590 (4) 0.354 (1)	−0.234 (1) −0.236 (1) −0.251 (3)	0.026 0.010 0.039
N6	0.3261 (5) 0.3226 (3) 0.318 (1)	0.4775 (4) 0.4734 (4) 0.468 (7)	0.123 (1) 0.1177 (9) 0.089 (4)	0.026 0.010 0.039
C2	0.5565 (6) 0.5585 (3) 0.558 (1)	0.0895 (6) 0.0934 (5) 0.095 (2)	0.185 (2) 0.188 (1) 0.195 (4)	0.026 0.010 0.039
C3	0.5733 (6) 0.5739 (3) 0.574 (1)	0.1762 (6) 0.1794 (5) 0.177 (2)	−0.047 (1) −0.040 (1) −0.043 (4)	0.026 0.010 0.039
C4	0.5161 (6) 0.5141 (4) 0.513 (2)	0.2685 (6) 0.2633 (5) 0.263 (2)	−0.055 (1) −0.059 (1) −0.058 (4)	0.026 0.010 0.039
C6	0.4323 (6) 0.4308 (4)	0.4248 (6) 0.4286 (4)	−0.184 (2) −0.178 (1)	0.026 0.010

Table 4 (cont.)

	<i>x</i>	<i>y</i>	<i>z</i>	U_{iso}
	0.431 (1)	0.432 (2)	−0.199 (4)	0.039
C7	0.3864 (6) 0.3843 (3) 0.389 (1)	0.4063 (6) 0.3970 (4) 0.404 (2)	0.044 (1) 0.044 (1) 0.042 (4)	0.026 0.010 0.039
C8	0.3986 (6) 0.3972 (3) 0.395 (1)	0.2925 (6) 0.2866 (4) 0.286 (2)	0.194 (1) 0.202 (1) 0.189 (4)	0.026 0.010 0.039
H3	0.606 (4) 0.580 (3) 0.588 (3)	−0.029 (4) −0.070 (4) −0.055 (4)	0.48 (1) 0.38 (1) 0.442 (9)	0.10 (3) 0.16 (3) 0.08 (1)
H31	0.638 (4) 0.645 (3) 0.651 (3)	−0.037 (4) −0.026 (4) −0.014 (3)	0.14 (1) 0.16 (1) 0.190 (9)	0.10 0.16 0.08
H5	0.527 (4) 0.534 (3) 0.534 (3)	0.367 (4) 0.388 (4) 0.387 (4)	−0.42 (1) −0.37 (1) −0.372 (8)	0.10 0.16 0.08
H6	0.312 (4) 0.307 (3) 0.303 (3)	0.544 (4) 0.537 (4) 0.524 (3)	−0.02 (1) −0.02 (1) −0.069 (9)	0.10 0.16 0.08
H61	0.284 (4) 0.280 (3) 0.280 (3)	0.435 (4) 0.425 (4) 0.433 (3)	0.21 (1) 0.20 (1) 0.21 (1)	0.10 0.16 0.08
H7	0.399 (4) 0.401 (3) 0.534 (3)	0.501 (4) 0.505 (4) 0.387 (4)	−0.54 (1) −0.53 (1) −0.372 (8)	0.10 0.16 0.08
H8	0.268 (4) 0.252 (3) 0.219 (3)	0.706 (4) 0.710 (4) 0.699 (4)	−0.14 (1) −0.120 (9) −0.119 (8)	0.10 0.16 0.08
H9	0.246 (4) 0.254 (3) 0.276 (3)	0.643 (4) 0.667 (4) 0.690 (4)	−0.42 (1) −0.42 (1) −0.351 (8)	0.10 0.16 0.08

weak in the final stages – biases the refined atomic coordinates. However, it was not possible to carry out the refinements without restraints, especially with X-ray laboratory and neutron data, as some of the distances and angles tended to unrealistic values. On the other hand the flexible use of bond restraints allows the molecule to suffer considerable conformational alterations during the course of refinement, leading to the correct solution even if preferred orientation is present. The case of the bond-restrained Rietveld refinement of (I) with the Guinier pattern I.1 is an illustrative example.

Comparing the possibilities offered by different powder instruments for crystal structure solution one may certainly conclude that the synchrotron powder diffractometer is the most suitable. Using synchrotron patterns I.2 and II.2 we were able to solve the structures of (I) and (II) using different software without any preliminary models of the molecule. However, at

present the most widely used powder instruments are laboratory X-ray diffractometers. The results of the present work clearly show the real and reliable possibility of molecular crystal structure solution from laboratory powder diffraction data. As a consequence of

the crystal structure solution we obtained the correct molecular structures for (I) and (II) distinguishing between several isomers which were indistinguishable by spectroscopic methods.

The possibilities of molecular crystal structure solution from neutron data are more limited compared with those from synchrotron and laboratory X-ray data for at least two reasons. First, owing to lower resolution of the neutron data we need to use a full initial molecular model including H atoms, as their scattering length – although negative – is of the same order of magnitude as the scattering lengths of the other atoms. Second, the large number of H atoms in organic molecules, like (I), decreases the signal-to-noise ratio owing to considerable incoherent scattering from the H atoms. Nevertheless, the principal uses of reliable crystal structure determination from neutron data are for cases when the organic powder is within a container impenetrable by X-rays, such as a gas pressure cell, or when complex or disordered hydrogen-bond patterns need to be resolved.

4. Conclusion

The results of crystal structure solution of two organic compounds from powder patterns measured at X-ray, synchrotron and neutron devices demonstrate the high

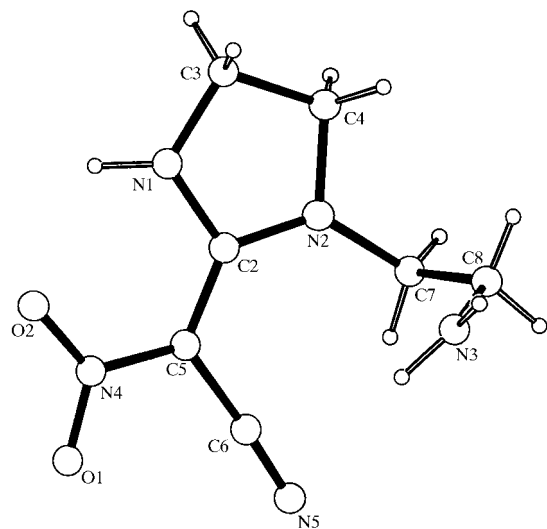


Fig. 4. The molecular structure of (I) with the atomic numbering.

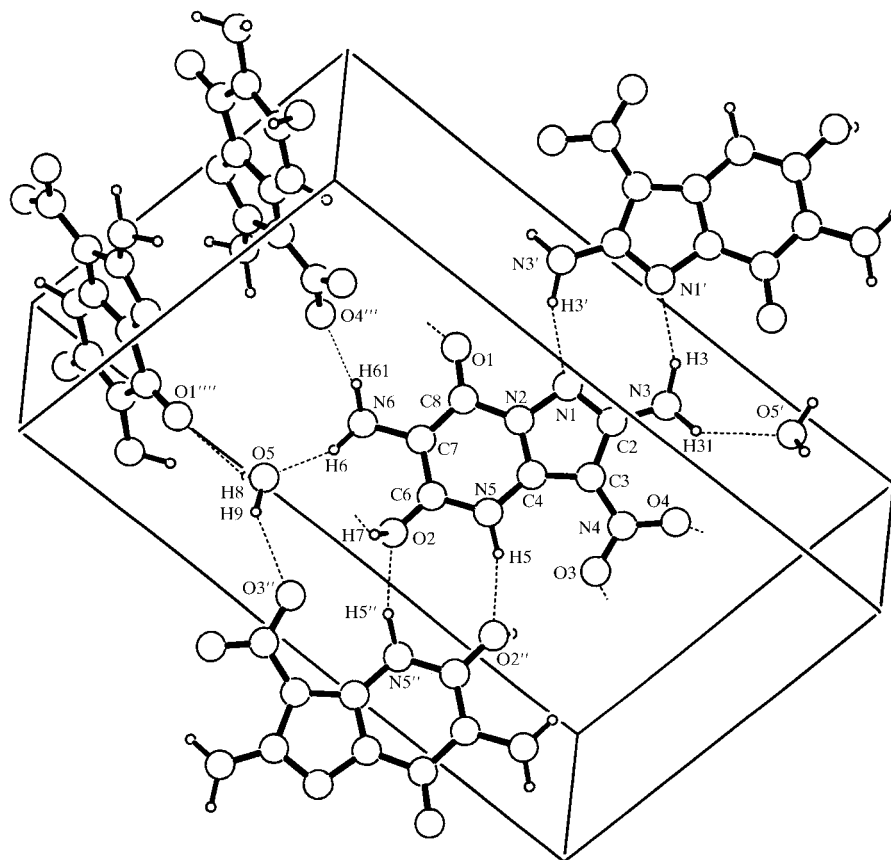


Fig. 5. The crystal packing of (II).

level of reproducibility and reliability of various powder software and equipment, with a certain preference for synchrotron facilities. It follows from the present work that the most effective way to solve the crystal structures of a series of organic compounds that can only be obtained in polycrystalline form is to use mainly an X-ray laboratory diffractometer, preferably in transmission mode, and to use synchrotron and neutron facilities in any 'non-standard' cases, e.g. for compounds with unknown molecular geometry, or when the unit cell is so large that indexing the pattern becomes the dominant problem.

The authors thank Dr A. V. Yatsenko and Dr N. C. Popa for helpful discussions. This work was supported by the Russian State Scientific and Technical Programs 'Neutron Investigations of Matter', the ORPHEE project (AIK & VVC), 'Contemporary Problems of Condensed Matter Physics' (VVC), the Netherlands Organization for Scientific Research (NWO) (VVC & VAT) and the Bundesministerium Forschung und Technologie, Bonn, Germany, project 'Transform' 01 KX9812 (VAM).

References

- Ahtee, M., Nurmela, M., Suortti, P. & Järvinen, M. (1989). *J. Appl. Cryst.* **22**, 261–268.
- Altomare, A., Cascarano, G., Giacovazzo, C., Guagliardi, A., Burla, M. C., Polidori, G. & Camalli, M. (1994). *J. Appl. Cryst.* **27**, 435–436.
- Bézar, J.-F. & Lelann, P. (1991). *J. Appl. Cryst.* **24**, 1–5.
- Beurskens, P. T., Beurskens, G., Bosman, W. P., de Gelder, R., Garcia-Granda, S., Gould, R. O., Israel, R. & Smits, J. M. M. (1996). *The DIRDIF96 Program System*. Crystallography Laboratory, University of Nijmegen, The Netherlands.
- Chernyshev, V. V. & Schenk, H. (1998). *Z. Kristallogr.* **213**, 1–3.
- David, W. I. F., Shankland, K. & Shankland, N. (1998). *Chem. Commun.* pp. 931–932.
- Dinnebier, R. E., Schneider, J., Rius, J. & Finger, L. (1997). *Ab initio Structure Determination of Molecular Solids from Powder Diffraction*. Fifth Workshop on Powder Diffraction. September 25–28, 1997. University of Bayreuth, Germany.
- Dollase, W. A. (1986). *J. Appl. Cryst.* **19**, 267–272.
- Egert, E. & Sheldrick, G. M. (1985). *Acta Cryst.* **A41**, 262–268.
- Giacovazzo, C. (1996). *Acta Cryst.* **A52**, 331–339.
- Harris, K. D. M., Johnston, R. L. & Kariuki, B. M. (1998). *Acta Cryst.* **A54**, 632–645.
- Järvinen, M. (1993). *J. Appl. Cryst.* **26**, 525–531.
- LeBail, A. (1998). *Structure Determination from Powder Diffraction – Database*, <http://flu.uiv.lemans.fr:8001/iniref.html>.
- Overbeek, O. & Schenk, H. (1978). *Computing in Crystallography*, edited by H. Schenk, R. Olthof-Hazekamp, H. van Koningsveld and G. C. Bassi, pp. 108–112. Delft University Press.
- Poojary, D. M. & Clearfield, A. (1997). *Acc. Chem. Res.* **30**, 414–422.
- Popa, N. C. (1998). *J. Appl. Cryst.* **31**, 176–180.
- Rius, J. & Miravittles, C. (1987). *J. Appl. Cryst.* **20**, 261–264.
- Rius, J. & Miravittles, C. (1988). *J. Appl. Cryst.* **21**, 224–227.
- Shankland, K., David, W. I. F. & Csoka, T. (1997). *Z. Kristallogr.* **212**, 550–552.
- Sheldrick, G. M. (1990). *Acta Cryst.* **A46**, 467–473.
- Sheldrick, G. M. (1993). *SHELXL93. Program for the Refinement of Crystal Structures*. University of Göttingen, Germany.
- Spek, A. L. (1992). *PLUTON92. Program for the Viewing, Analysis and Presentation of Molecular Structures*. University of Utrecht, The Netherlands.
- Stewart, J. J. P. (1990). *MOPAC6.0*. QCPE Program No. 455. Quantum Chemistry Program Exchange, Department of Chemistry, Indiana University, Bloomington, IN, USA.
- Toraya, H. (1986). *J. Appl. Cryst.* **19**, 440–447.
- Tremayne, M., Kariuki, B. M. & Harris, K. D. M. (1996). *J. Appl. Cryst.* **29**, 211–214.
- Visser, J. W. (1969). *J. Appl. Cryst.* **2**, 89–95.
- Visser, J. W. (1986). *Powder Diffr.* **1**, 66–76.
- Werner, P.-E., Eriksson, L. & Westdahl, M. (1985). *J. Appl. Cryst.* **18**, 367–370.
- Yatsenko, A. V., Chernyshev, V. V., Zhukov, S. G., Sonneveld, E. J. & Schenk, H. (1999). *Powder Diffr.* **14**, 133–135.
- Zlokazov, V. B. (1992). *J. Appl. Cryst.* **25**, 69–72.
- Zlokazov, V. B. & Chernyshev, V. V. (1992). *J. Appl. Cryst.* **25**, 447–451.